Non-ideal Modifications of Three-dimensional Equilibrium and Resistive Wall Mode Stability Models in DIII-D

H. Reimerdes[1], J.W. Berkery[1], M.J. Lanctot[1], M.S. Chu[2], A.M. Garofalo[2], J.M. Hanson[1], Y. In[3], R.J. La Haye[2], Y.Q. Liu[4], G. Matsunaga[5], G.A. Navratil[1], M. Okabayashi[6], S.A. Sabbagh[1], and E.J. Strait[2]

[1]Columbia University, New York, New York 10027-6902, USA
[2]General Atomics, P.O. Box 85608, San Diego, California 92186-5608, USA
[3]FAR-TECH, Inc., San Diego, California 92121, USA
[4]Culham Science Centre for Fusion Energy, Culham Science Centre, Abingdon, UK
[5]Japan Atomic Energy Agency, Naka 311-0193, Japan
[6]Princeton Plasma Physics Laboratory, Princeton, New Jersey 08543-0451, USA

e-mail: reimerdes@fusion.gat.com

Abstract. Recent DIII-D experiments deliver strong evidence for the importance of kinetic modifications of ideal MHD three-dimensional (3D) equilibrium and resistive wall mode (RWM) stability models at high plasma pressure. Magnetic measurements of the plasma response to externally applied long-wavelength perturbations of the order of $\delta B/B_T \leq 10^{-3}$ show that linear ideal MHD can only describe three-dimensional equilibria for plasma pressures up to 80% of the ideal MHD stability limit. At higher pressure, the observed stability of the RWM over a wide range of plasma rotation profiles and the measured dependence of the plasma response on plasma pressure and rotation are both explained by including wave-particle resonances due to the quasi-static perturbation of the equilibrium field in the model. The DIII-D results highlight the necessity to extend the original kinetic RWM stability model [A. Bondeson, M.S. Chu, Phys. Plasmas **3**, 3013 (1996)] by including the precession motion of trapped particles [B. Hu, R. Betti, Phys. Rev. Lett. **93**, 105002 (2004)] as well as the effect of trapped fast ions. Experimental validation of these kinetic effects is essential in developing confidence in predictions for reactor scenarios that rely on wall-stabilization, such as the steady-state scenario in ITER.

1. Introduction

Three-dimensional (3D) equilibria and resistive wall mode (RWM) stability are two important aspects of the optimization of the tokamak approach towards fusion energy. Recent DIII-D experiments show the important role of kinetic modifications of ideal MHD models in both these areas.

Three-dimensional equilibria arise from non-axisymmetric currents outside the plasma. If the external non-axisymmetric currents are unintentional or unavoidable, the corresponding non-axisymmetric field is referred to as an error field. The resulting non-axisymmetry of the plasma can brake the toroidal plasma rotation below a tolerable level and thereby determine the error field tolerance of a tokamak [1,2]. Taking into account how the plasma responds to the external field has been critical for the qualitative understanding of the error field tolerance in present devices [3]. Recently external non-axisymmetric fields have also been intentionally applied in order to improve the plasma performance by for example suppressing edge localized modes (ELMs) [4] or driving rotation [5]. The knowledge of the 3D equilibrium is a prerequisite for the understanding of all of these processes. Notably the effects that modify ideal MHD theory of 3D equilibria are also the physics basis for the stabilization of the RWM in high β plasmas. RWM stabilization can allow for a substantial gain in plasma pressure and is therefore very attractive for reactor scenarios. Sustained operation in this wall-stabilized regime has been demonstrated at high [6] and low plasma rotation [7], but the extrapolation to a reactor requires a quantitative understanding of the stabilizing processes.

While both 3D equilibria and RWMs are important in different contexts, they share a similar physics basis. Both constitute quasi-static deformations of the flux surfaces. In the case of the 3D equilibrium the rotation frequency of the perturbation is determined by the rotation of the external field, which in the case of error fields is generally static. In the case of the RWM the plasma determines the rotation frequency of the perturbation, but it cannot significantly exceed the inverse of the characteristic resistive time of the wall. For DIII-D the characteristic wall time of a typically $n=1$ kink mode perturbation is of the order of $\tau_W \approx 3$ ms corresponding to approximately 300 radians/second. This time-scale is slow with respect to most other processes, such as plasma rotation and particle motions and the RWM can therefore also be regarded as a quasi-static perturbation. The similarity in the physics basis has already been exploited by using the 3D response of plasmas to externally applied non-axisymmetric fields as an active measurement of the RWM stability [8,9].

Motivated by the observation of transient wall-stabilization in rotating DIII-D plasmas [10], it was suggested that the plasma flow through the perturbed field leads to dissipation, which, in the case of the RWM, can linearly stabilize the mode [11]. Subsequently, a kinetic stabilization mechanism was proposed [12], and later extended to low frequencies [13]. Recent observation of the unstable RWM at intermediate plasma rotation in NSTX supports the relevance of the kinetic effects [14,15]. The DIII-D results presented in this paper yield direct evidence for the importance of the predicted kinetic modifications of ideal MHD 3D equilibria and RWM stability.

In Sec. 2 it is shown that a linear ideal MHD model adequately describes macroscopic features of the 3D equilibria over a wide parameter range, but fails at high plasma pressure and at low rotation. In Sec. 3 it is shown that the modification of ideal MHD at high β is also manifested in the observed RWM stability. The kinetic modeling is consistent with the experiment, if fast ions from the strong neutral beam injection heating are included. Section 4 shows how the kinetic resonances are visible in the plasma response to externally applied fields, yielding direct evidence for the relevance of kinetic effects for 3D equilibria at high β as well as for RWM stability. Section 5 summarizes the results.

2. Applicability of a Linear Ideal MHD 3D Equilibrium Model

A linear ideal MHD 3D equilibrium model is tested by comparing predictions of the plasma response to externally applied non-axisymmetric fields with DIII-D measurements. It is found that the model is adequate to describe the plasma response over a wide range of plasma pressures and plasma rotations, but fails at high plasma pressure and at low plasma rotation.

Ideal MHD, which is widely used to describe axisymmetric tokamak equilibria, can be adapted to calculate 3D equilibria. An external 3D magnetic field perturbs the force balance of the 2D equilibrium and the plasma is displaced until a new 3D equilibrium is found. In an ideal conducting plasma this leads to non-axisymmetric currents inside the plasma including sheet currents on resonant surfaces, which screen the resonant component of the external field. A linear ideal MHD 3D equilibrium model is included in the MARS-F code [16].

The present DIII-D experiments use the I-coil, which consists of two toroidal arrays above and below the outboard midplane with six saddle coils each, to apply external $n=1$ and $n=3$ fields of the order of $\delta B/B_T \leq 10^{-3}$, Fig. 1(a). The plasma response $\delta \mathbf{B}_{s,n}^{plas}$, which is the component of the perturbed field generated by perturbed currents inside the plasma, is

obtained from magnetic measurements with toroidal arrays of poloidal and radial field sensors (with the index s denoting the array), also shown in Fig. 1(a), by subtracting the measured vacuum coupling. In this article bold symbols denote the complex notation of quantities with an amplitude and a toroidal phase. While both arrays can resolve the amplitude and toroidal phase of the $n=1$ component of the magnetic field, only the poloidal field probe array is adequate to measure amplitude and phase of the $n=3$ component. The signal-to-noise ratio of the magnetic measurement can be improved by slowly rotating the external field in the toroidal direction and extracting the response at the applied frequency using Fourier techniques. The rotation frequency is chosen to be slow with respect to all other relevant time scales including the wall time. However, due to the six-fold geometry of the I-coil a rotating field can only be applied for $n<3$.

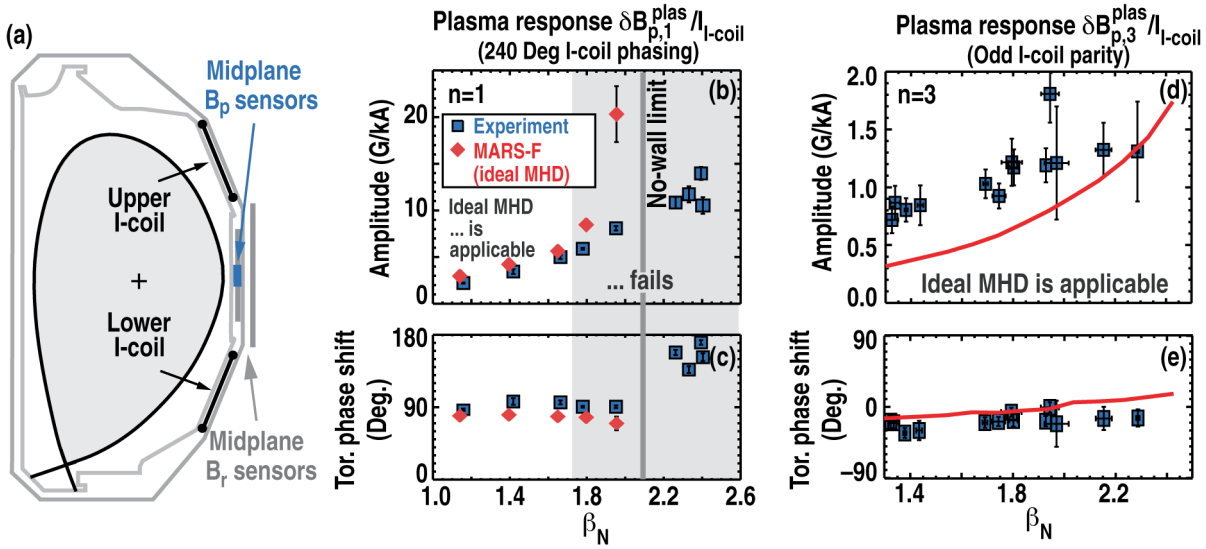

FIG. 1. (a) Poloidal cross-section of DIII-D showing plasma shape, I-coil geometry and the location of magnetic sensor arrays. (b-e) Comparison of the measured amplitude (b,d) and toroidal phase shift (c,e) of the plasma response (squares) to external $n=1$ (b,c) and $n=3$ (d,e) I-coil fields with linear ideal MHD modeling using MARS-F (diamonds, solid lines). The shaded region indicates the β_N range where ideal MHD fails to describe the measurements.

2.1 Beta Dependence of the Plasma Response

The β-dependence of the plasma response to externally applied quasi-static $n=1$ and $n=3$ fields is investigated in two series of similar lower single null (LSN) H-mode discharges [5,17]. In both series dominant tangential neutral beam injection (NBI) heating results in fast toroidal plasma rotation.

For the investigation of $n=1$ equilibria a phase difference of the $n=1$ current in the upper and lower I-coil arrays of $\Delta\phi_{I-coil} = 240$ degrees is chosen because it couples well to the kink mode [18]. The external field is rotated with a frequency of $f_{ext} = 10$ Hz in the direction of the plasma current. The scan of β_N from 1.1 to 2.4 yields an increase of the plasma response $\delta\mathbf{B}^{plas}_{p,1}$ with β_N, Fig. 1(b). The magnetic measurements are compared with predictions by the linear ideal MHD model implemented in the MARS-F code [16]. For values of β_N up to approximately 1.7, which corresponds to approximately 80% of the ideal MHD no-wall limit, the predictions of the ideal MHD model are in good agreement with the measured amplitude and phase shift of $\delta\mathbf{B}^{plas}_{p,1}$, Fig. 1(b,c) [17]. Note that the phase shift between plasma response and currents in the I-coils depends on details of the coupling. For higher values of β_N the

model increasingly overestimates the amplitude of the plasma response. Above the no-wall limit the ideal MHD model is obviously not adequate since it predicts a growing RWM. Additionally, the linear ideal MHD prediction of a small plasma response to the same externally applied $n = 1$ I-coil field in low β L-modes is consistent (within the uncertainty of the magnetic measurements) with no measurable $\delta\mathbf{B}_{p,1}^{plas}$. The consistency only holds as long as the plasma rotates and the external field does not penetrate.

Similarly, $n = 3$ equilibria are generated by applying an $n = 3$ field. Here, an odd $n = 3$ parity is used, where the coils of the upper and lower I-coil arrays have opposite currents. The uncertainty of the $n = 3$ plasma response measurement is higher than the $n = 1$ measurement, since it is extracted from the response to a step function rather than by Fourier analysis over several hundred milliseconds. The $n = 3$ plasma response measured with the midplane poloidal field sensors $\delta\mathbf{B}_{p,3}^{plas}$ increases with β_N, Fig. 1(d). The ideal MHD predictions by the MARS-F code are in reasonable agreement with the measured amplitude and phase of $\delta\mathbf{B}_{p,3}^{plas}$ over the entire range of probed values of β_N from 1.3 to 2.3, Fig. 1(d,e). The probed range is thereby significantly lower than the estimated ideal MHD no-wall limit set by the $n = 3$ mode of $\beta_{N,nw}^{n=3} \approx 2.8$ obtained with the ideal MHD stability code DCON [19]. The observed increase of the deviations between model and measurements with higher toroidal mode numbers is not unexpected, since their stability increasingly depends on the evolution of the pressure profile within the ELM cycle (approximately 5 millisecond in these discharges). In this study the pressure profile measurements that serve as a constraint for the equilibrium reconstruction as well as the plasma response measurements have been averaged over several hundred milliseconds and hence many ELM cycles.

2.2 Rotation Dependence of the Plasma Response

Plasma rotation can modify the ideal MHD description of 3D equilibria in several ways. Most importantly rotation is needed in order to uphold screening currents on resonant surfaces which otherwise would dissipate and lead to magnetic islands. Rotation exceeding the inverse of the typical reconnection time τ_{rec} is therefore a prerequisite of the ideal MHD model.

The rotation in a LSN H-mode with tangential NBI heating at $\beta_N = 1.6$, similar to the discharges used above, is slowed by increasing the amplitude of an $n = 1$ I-coil field. In this example the plasma rotation, evaluated at the q=2 surface, slows from 25 krad/s to 12 krad/s without any significant deviations of the measured plasma response from the linear ideal MHD prediction, Fig. 2. At these values of rotation and β_N non-ideal effects are negligible. Increasing the amplitude of the external field further causes a rapid rotation collapse to nearly zero rotation, which is interpreted as a bifurcation in the torque balance. After the rotation collapse electron temperature measurements clearly show evidence of an island at the $q = 2$ surface [18]. The observation of the island is consistent with penetration of the external field since the plasma rotation is now comparable with the inverse of τ_{rec}, which in the visco-resistive limit [1] is estimated to be approximately 25 milliseconds. This limit of validity of the ideal MHD 3D equilibrium model is also seen by a significant increase of the measured plasma response over the linear ideal MHD prediction, Fig. 2.

While the comparison of the magnetic measurement with the linear ideal MHD model yields good agreement over a wide range of β_N and plasma rotation, there can still be local deviations from ideal MHD. One indication of local deviations from ideal MHD is the measurable toroidal torque that results from the external 3D field [18]. Another indication is a

splitting of the strike points in the divertor heat and particle flux, which implies a breaking of the nested flux surface topology near the separatrix [20].

3. RWM Stabilization

Sustained operation above the ideal MHD no-wall limit demonstrates the importance of non-ideal effect. The wide range of stable rotation profiles is explained by a kinetic stability model, which reveals a significant contribution from fast neutral beam ions to the RWM stability.

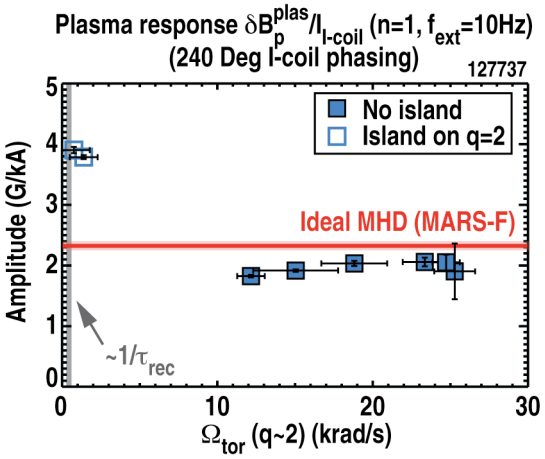

FIG. 2. Measured plasma rotation dependence of the plasma response $\delta \mathbf{B}_{p,1}^{plas}$ to a quasi-static $n=1$ I-coil field (squares) and the corresponding ideal MHD prediction (horizontal line). Island formation at the $q=2$ surface is indicated (open symbols) and an estimate of the inverse of the reconnection time τ_{rec} marked (vertical line).

DIII-D can routinely exceed the ideal MHD no-wall limit and allows for sustained operation up to the ideal wall limit [6]. Since ideal MHD predicts the growth of an RWM as soon as the plasma exceeds the no-wall stability limit, stable operation above the no-wall limit directly demonstrates the importance of non-ideal effects. Furthermore, stable operation can be achieved even at very low plasma rotation, as long as the error field is sufficiently well corrected [7]. Figure 3(a-c) shows an example of a low-rotation discharge in the wall-stabilized regime. Ideal MHD stability calculations based on an equilibrium at $\beta_N \approx 2.3$ (t = 3.0 s) using DCON yield a no-wall limit of $\beta_{N,nw}$ = 1.95 and an ideal wall limit of $\beta_{N,iw}$ = 2.75. In a set of similar discharges with the NBI torque T_{NBI} ranging from 1.5 Nm to 8.0 Nm various experimentally stable ω_E rotation profiles, shown in Fig. 3(d), have been obtained. The toroidal rotation associated with the radial electric field $\omega_E \equiv -d\phi/d\psi$, with ϕ being the electrostatic potential and ψ the poloidal flux, is derived from poloidal and toroidal rotation measurements by charge exchange recombination spectroscopy using C VI emission.

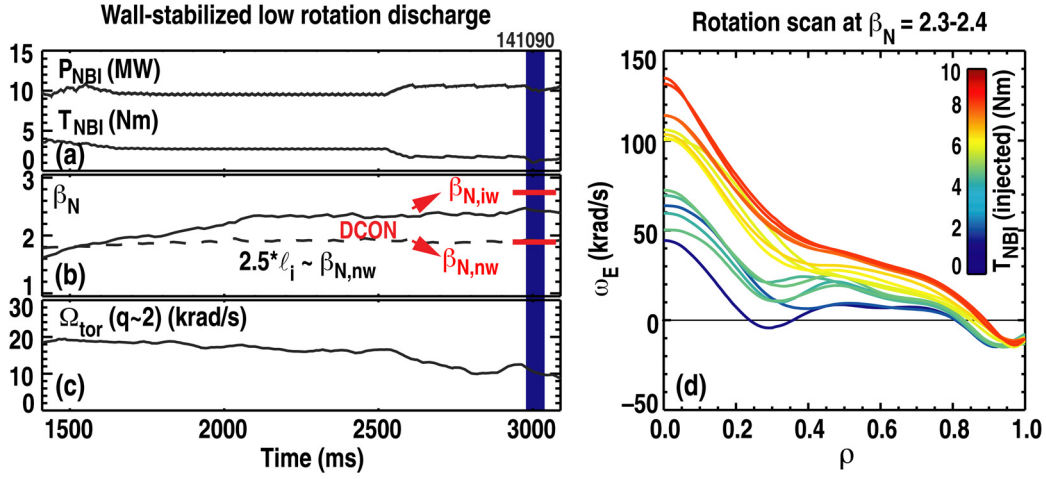

FIG. 3. Stable operation with (a) high NBI heating power P_{NBI} and low torque T_{NBI} resulting in (b) a value of β_N above the no-wall limit and (c) low toroidal plasma rotation. (d) A shot-to-shot scan of T_{NBI} at constant β_N yields a wide range of stable ω_E rotation profiles.

The set of stable rotation profiles, Fig. 3(d), is used to test the kinetic RWM stability model implemented in the MISK code [14]. In addition to resonances with the transit frequency of passing particles and the bounce frequency of trapped particles, MISK also includes the effect of precessing trapped ions [13] and the effect of fast ions from the NBI heating [21]. The MISK code uses a perturbative approach based on the marginally unstable kink-mode structure to calculate the RWM growth rate γ_{RWM} and RWM rotation frequency ω_{RWM}, both normalized with the inverse of the characteristic decay time τ_W of induced currents in the resistive wall. A systematic rotation scan, shown in Fig. 4(a), is generated by fitting a low order polynomial to the T_{NBI} dependence of the experimental rotation, Fig. 3(d), at each radius. Taking into account only thermal particles the kinetic RWM stability model implemented in the MISK code leads to stability at low plasma rotation $[\omega_{\mathrm{E}}\tau_{\mathrm{A}}(q=2) < 0.6\%]$, when precessing trapped ions resonate in the perturbed magnetic field, and at higher rotation $[\omega_{\mathrm{E}}\tau_{\mathrm{A}}(q=2) > 1.2\%]$, when the bounce motion of trapped particles and the transit motion of circulating particles begin to become important. However thermal particles alone are not sufficient to explain the observed stability over the entire range of rotation profiles, Fig. 4(b). Adding the contribution of trapped fast ions, which constitute approximately 20% of the kinetic energy of these plasmas, stabilizes the RWM over the entire range of rotation profiles $[\omega_{\mathrm{E}}\tau_{\mathrm{A}}(q=2) \sim 0\%–2\%]$, Fig. 4(b), consistent with DIII-D observations. The importance of energetic ions for RWM stability is further supported by observations on DIII-D and JT-60U that fishbone like modes, which quickly redistribute energetic ions, can trigger RWMs [22,23]. The strong dependence of the kinetic stabilization on the plasma rotation with respect to various particle frequencies is consistent with previous predictions for JET [9] and NSTX [14].

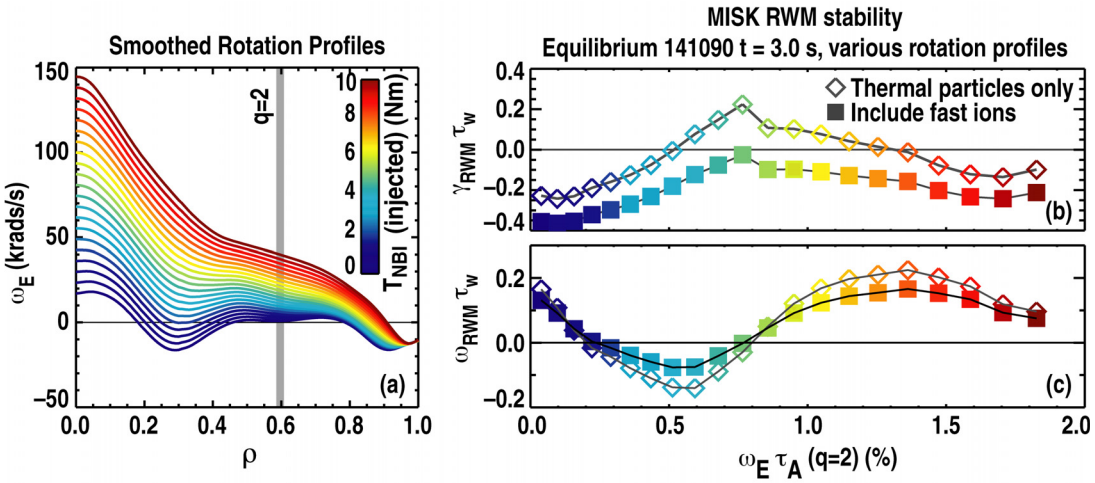

FIG. 4. (a) Smoothed stable ω_{E} rotation profiles and kinetic calculations of (b) the RWM growth rate and (c) RWM rotation frequency with (squares) and without (diamonds) energetic ions using the MISK code as a function of ω_{E} at q=2 normalized with the inverse Alfvén time.

4. Manifestation of Particle Resonance in the 3D Equilibrium Response

Measurements of the plasma response to external non-axisymmetric fields in plasmas above the ideal MHD no-wall stability limit also yield direct evidence for the importance of the precession frequency of trapped ions.

The set of discharges with various rotation profiles shown in Fig. 3(d) is probed with a low amplitude slowly rotating ($f_{\mathrm{ext}} = 20$ Hz) $n = 1$ I-coil field. Magnetic measurements yield the

largest amplitude of the plasma response $\delta\mathbf{B}_{r,1}^{plas}$, when $\omega_E\tau_A(q=2) \approx 0.9\%$, which is in the gap between typical precession and bounce frequencies of trapped particles, Fig. 5(a). The amplitude decreases at higher as well as at lower plasma rotation. The largest phase shift, with the plasma response trailing the currents in the coil by 70 Degrees, is observed, when $\omega_E\tau_A(q=2) \approx 0.6\%$, Fig. 5(b).

The amplitude and phase of the plasma response can be linked to the RWM growth rate and mode rotation frequency by a single-mode model [24],

$$\delta\mathbf{B}_s^{plas} = \frac{(\hat{\gamma}_{RWM}\tau_W + 1)}{(i\omega_{ext}\tau_W - \hat{\gamma}_{RWM}\tau_W)(i\omega_{ext}\tau_W + 1)} M_{sc}^* \mathbf{I}_c \quad , \qquad (1)$$

where $\hat{\gamma}_{RWM} \equiv \gamma_{RWM} + i\omega_{RWM}$ is the complex RWM growth rate, $\mathbf{I}_c$ the current in the non-axisymmetric coil and M_{sc}^* an effective mutual inductance. The value of M_{sc}^* depends mainly on the geometry of the coil, the mode structure and the geometry of the magnetic sensors used. A scan of the rotation $f_{ext} = \omega_{ext}/(2\pi)$ of the I-coil field in similar shaped plasmas previously yielded $M_{sc}^* = (1.0 + 0.3i)G/kA$ [24]. The comparison of measured and modeled dependence of the amplitude and the phase of the plasma response on plasma rotation, shown in Fig. 5, yields good agreement. The model reproduces in particular the largest amplification for the rotation profiles with $\omega_E\tau_A(q=2) \approx 1\%$ as well as the largest toroidal phase shift at a distinctively lower plasma rotation. Due to a large uncertainty in the coupling coefficient M_{sc}^* the good quantitative agreement between measurements and modeling may be partially fortuitous. Further uncertainties arise from the perturbative nature of the MISK modeling [21], from uncertainties in the fast ion content and from the simplified assumption for the fast ion distribution function in the MISK code. The main result is the reproduction of the qualitative characteristics of the plasma rotation dependence of the plasma response by the kinetic stability model. The features at low rotation are directly related to the resonance with the precession frequency of the trapped (thermal) ions, revealing that the predicted effects are indeed relevant for RWM stability and hence 3D equilibria at high β.

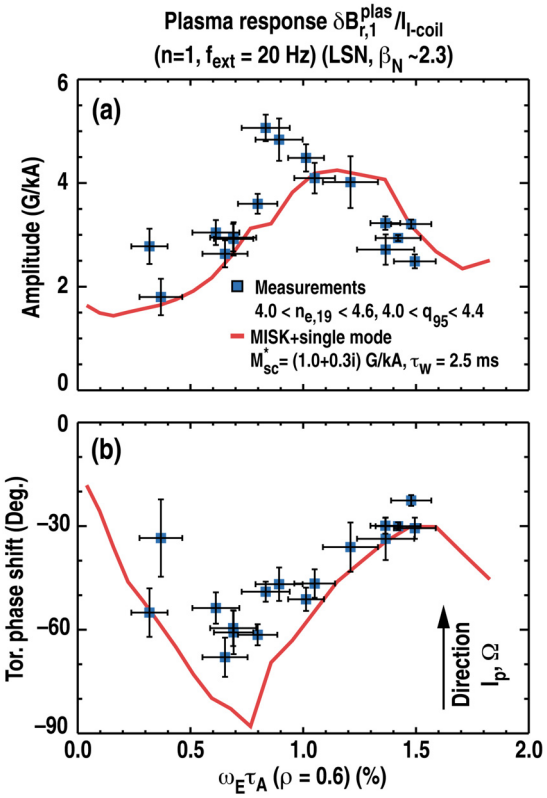

FIG. 5. Measured (squares) and modeled (line) dependence on the normalized ω_E at $\rho = 0.6$ of (a) the amplitude and (b) toroidal phase shift of the plasma response $\delta\mathbf{B}_{r,1}^{plas}$ to a slowly rotating (f_{ext} = 20 Hz) externally applied n=1 I-coil field in a set of similar discharges at $\beta_N \approx 2.3 > \beta_{N,nw}$

5. Summary

Three-dimensional equilibria and RWM stability, which both constitute a quasi-static perturbation of the axisymmetric magnetic configuration, share a similar physics basis. While

the linear ideal MHD model implemented in the MARS-F code [16] is adequate to describe the global features of the plasma response to externally applied long-wavelength perturbations with $\delta B/B_T \leq 10^{-3}$ in rotating plasmas up to intermediate values of β_N, non-ideal modifications become apparent even before β_N exceeds the ideal MHD no-wall stability limit [17]. Above the no-wall limit the observed RWM stability over a wide range of β_N and plasma rotation manifests the importance of non-ideal effects. The kinetic stability model implemented in the MISK code [14] explains the wide range of stable rotation profiles in DIII-D, but has to include the contribution of trapped fast ions from the NBI heating. Direct evidence for the importance of the precession frequency of trapped thermal ions is obtained from a measurement of the rotation dependence of the amplitude and phase of the plasma response to externally applied $n = 1$ fields.

Modifications of ideal MHD are the physics basis for passive RWM stabilization, which is very attractive for a reactor since it increases the attainable β_N, and thereby fusion performance, without the need for a magnetic feedback system. The present DIII-D results identify the relevant physics processes, but in order to gain confidence in any extrapolation of the potential of passive RWM stabilization from today's NBI heating dominated experiments to a burning plasma (e.g. [13,21,25]), the qualitative understanding must evolve into a quantitative understanding.

This work was supported in part by the US Department of Energy under DE-FG02-89ER53297, DE-FG02-06ER84442, DE-FC02-04ER54698, and DE-AC02-09CH11466.

References

[1] FITZPATRICK, R., Nucl. Fusion **33** (1993) 1049
[2] BOOZER, A.H., Phys. Rev. Lett. **86** (2001) 5059
[3] PARK, J.-K., et al., Phys. Rev. Lett. **99** (2007) 195003
[4] EVANS, T.E., et al., Nature Phys. **2** (2006) 419
[5] GAROFALO, A.M., et al., Phys. Rev. Lett. **101** (2008) 195005
[6] GAROFALO, A.M., et al., Phys. Rev. Lett. **89** (2002) 235001
[7] REIMERDES, H., et al., Phys. Rev. Lett. **98** (2007) 055001
[8] REIMERDES, H., et al., Nucl. Fusion **45** (2005) 368
[9] CHAPMAN, I.T., et al., Plasma Phys. Control. Fusion **51** (2009) 055015
[10] STRAIT, E.J., et al., Phys. Rev. Lett. **74** (1995) 2483
[11] BONDESON A. and WARD, D.J., Phys. Rev. Lett. **72** (1994) 2709
[12] BONDESON A. and CHU, M.S., Phys. Plasmas **3** (1996) 3013
[13] HU, B. and BETTI, R., Phys. Rev. Lett. **93** (2004) 105002
[14] BERKERY, J.W., et al., Phys. Rev. Lett. **104** (2010) 035003
[15] SABBAGH, S.A., et al., "Resistive Wall Mode Stabilization and Plasma Rotation Damping Considerations for Maintaining High β Plasma Discharges in NSTX," this conference, EXS/5-5
[16] LIU, Y.Q., et al., Phys. Plasmas **7** (2000) 3681
[17] LANCTOT, M.J., et al., Phys. Plasmas **17** (2010) 030701
[18] REIMERDES, H., et al., Nucl. Fusion **49** (2009) 115001
[19] GLASSER A. and CHANCE, M.S., Bull. Am. Phys. Soc. **49** (1997) 1848
[20] SCHMITZ, O., et al., "Key Results from the DIII-D/TEXTOR Collaboration on the Physics of Stochastic Boundaries Projected to ELM Control at ITER," this conference, EXD/P3-30
[21] BERKERY, J.W., et al., Phys. Plasmas **17** (2010) 082504
[22] OKABAYASHI, M., et al., Nucl. Fusion **49** (2009) 125003
[23] MATSUNAGA, G., et al., Phys. Rev. Lett. **103** (2009) 045001
[24] REIMERDES, H., et al., Phys. Rev. Lett. **93** (2004) 135002
[25] LIU, Y.Q., Nucl. Fusion **50** (2010) 095008